Late Holocene Peléan-style eruption at Tacaná volcano, Mexico and Guatemala: Past, present, and future hazards

J.L. Macías*
J.M. Espíndola
A. García-Palomo
Instituto de Geofísica, Universidad Nacional Autónoma de México, Coyoacán 04510, México D.F., México

K.M. Scott
Cascades Volcano Observatory, 5400 MacArthur Boulevard, Vancouver, Washington 98661, USA

S. Hughes
Department of Geology, State University of New York, 876 Natural Science Complex, Buffalo, New York 14260, USA

J.C. Mora
Dipartimento di Scienze della Terra, Università degli Studi di Firenze, Firenze, Italia

ABSTRACT

Tacaná volcano, located on the border between Mexico and Guatemala, marks the northern extent of the Central American volcanic chain. Composed of three volcanic structures, it is a volcanic complex that has had periodic explosive eruptions for at least the past 40 k.y. The most recent major eruption occurred at the San Antonio volcano, the youngest volcanic edifice forming the complex, about 1950 yr ago. The Peléan style eruption, issued from the southwest part of the dome, and swept a 30° sector with a hot block and ash flow that traveled about 14 km along the Cahoacán ravine. Deposits from this event are well exposed around the town of Mixcun and were therefore given the name of that town, the Mixcun flow deposit. The Mixcun flow deposit is, in the channel facies, a light gray, massive, thick (>10 m), matrix-supported unit with dispersed lithic clasts of gravel to boulder size, divisible in some sections into a variable number of flow units. The overbank facies is represented by a thin (<1 m), massive, matrix-supported unit. In both of these facies the deposit has disseminated charcoal, fumarolic pipes, and juvenile lithics with cooling joints. The Mixcun flow deposit contains clasts of (1) light gray, dense andesite, (2) dark gray, glassy and banded andesite, and (3) minor altered red andesite from the edifice, set in a matrix of sand and silt. The Mixcun flow deposit covers an area of at least 25 km^2 and has a minimum estimated volume of 0.12 km^3. Basaltic-andesite inclusions (54% SiO_2) and various signs of disequilibrium in the mineral assemblage of the two-pyroxene andesitic products (60%–63% SiO_2) suggest that magma mixing may have triggered the eruption. Following deposition of the Mixcun flow deposit andesitic to dacitic (62%–64% SiO_2) lava flows were extruded and a dacitic dome (64.4% SiO_2) at the San Antonio summit formed. Syneruptive and posteruptive lahars flooded the main drainages of the Cahoacán and Izapa-Mixcun valleys in the area of the present city of Tapachula (population 250 000) and the pre-Hispanic center of Izapa. Three radiocarbon ages date this event between A.D. 25 and 72 (range ±1σ, 38 B.C.–A.D. 216), which correlates with a halt in construction at Izapa (Hato phase of ca. 50 B.C.–A.D. 100), probably due to temporary abandonment of the city caused by lahars. Another similar event would produce extensive damage to the towns (population of about 68 000 people) now built upon the Mixcun flow deposit. The main summit of Tacaná volcano continues to show signs of fumarolic activity; the most recent period of activity in 1985–1986 culminated in a minor phreatic explosion.

Keywords: archaeology, Chiapas Mexico, magma, mixing, Peléan-type eruption.

INTRODUCTION

Tacaná volcano (lat 15°8′N, long 92°9′W) is in the State of Chiapas in southern Mexico and in the San Marcos Department in Guatemala. Shared by the two countries, the summit delineates the international boundary. The volcano is the most northern of the Central American Volcanic Arc (Fig. 1A). For several small towns and coffee plantations, this volcano constitutes a hazard to the population of the surrounding area and their economic activity. The city of Tapachula, Chiapas (250 000 inhabitants), the second largest in the state, is located 30 km southwest of the volcano's summit. Although no historical explosive eruptions are known, recent periods of fumarolic and seismic upheaval have reminded us of the potential. Bergeat (1894) and Sapper (1927) published the first known historical information on the activity of the volcano. In the first detailed description of Tacaná, Böse (1903) reported accounts from local residents who claimed that ash emissions had occurred in 1855 and 1878. In 1949 and 1950 the volcano resumed seismic and fumarolic activity, during which a wide area to the southwest of the summit developed fumaroles (Müllerried, 1951). After a series of earthquakes that began in December 1985, on May 7, 1986, an earthquake swarm with epicenters on the southwest flank of the volcano was followed by a phreatic explosion that generated a fumarole (De la Cruz-Reyna et al., 1989; Mercado and Rose, 1992). Although basic monitoring was undertaken during this crisis, it did not continue thereafter, nor were systematic volcanologic studies carried out.

The most complete geological study in the region to date was made by geologists from the Comisión Federal de Electricidad, Mexico's National Power Company, as part of their ongoing research on the potential of geothermal areas in Mexico (De la Cruz and Hernández, 1985). De la Cruz and Hernández (1985) described and

*E-mail: macias@tonatiuh.igeofcu.unam.mx.

GSA Bulletin; August 2000; v. 112; no. 8; p. 1234–1249;14 figures; 4 tables.

mapped three pyroclastic flow deposits of Quaternary age which they labeled, from youngest to oldest, as Qt1, Qt2, and Qt3. Charcoal samples found within unit Qt3 (Espíndola et al., 1989, 1993) defined its age as 38 000 yr B.P. De Cserna et al. (1988), and Mercado and Rose (1992) published geologic maps that focused on volcanic deposits and their hazard implications, based mostly on photointerpretation.

The lack of a detailed volcanologic study motivated us to begin research on the volcanic history of Tacaná. We present in this study details of the latest large eruption of the volcano that produced a series of block and ash-flow deposits that are well exposed and quarried around Mixcun, a small town ~14 km south-southwest from the volcano summit. We present the distribution, stratigraphy, and sedimentology of the Mixcun flow deposit as a first step to understand the eruptive style of the event. An interpretation of the triggering mechanisms of the eruption through petrographic and chemical analysis of the juvenile products is also given. Finally, we discuss the eruption's impact on the nearby pre-Hispanic settlement of Izapa, and try to gain a general insight into the hazard that a potential future event would pose to the surrounding populations.

GEOLOGIC SETTING AND MORPHOLOGY

Tacaná volcano is built within the remains of a 9 km semicircular caldera structure surrounded by Paleozoic granitic rocks and Tertiary granodiorites and tonalites that vary in age from 15 to 29 Ma (Mujica, 1987). The local basement of the volcano consists of late Tertiary–Quaternary ignimbrites, suggesting that the surrounding structure is in fact an older caldera (Fig. 1B). The volcano rises more than 2000 m over the granitic and ignimbrite basement and is crowned by three volcanic edifices: Chichuj (3800 m a.s.l. [above sea level]), the main summit, which local people distinguish as the proper Tacaná (4060 m a.s.l.), and San Antonio (3700 m a.s.l.). Hereafter, we will refer to the overall volcano edifice as the Tacaná volcanic complex (Fig. 2). Eruptions of the Tacaná volcanic complex have taken place at these different volcanoes that migrated from the east-northeast (Chichuj) to the west-southwest (San Antonio). This volcanic structure is similar to the geometry of pair volcanoes in northern Central America (Halsor and Rose, 1988). Historic and modern fumarolic activity in the area has occurred around the Tacaná and San Antonio volcanoes. The main summit, Tacaná, consists of a crater about 600 m in diameter, open to the northwest, which contains an andesitic dome about 80 m high. Rising above this

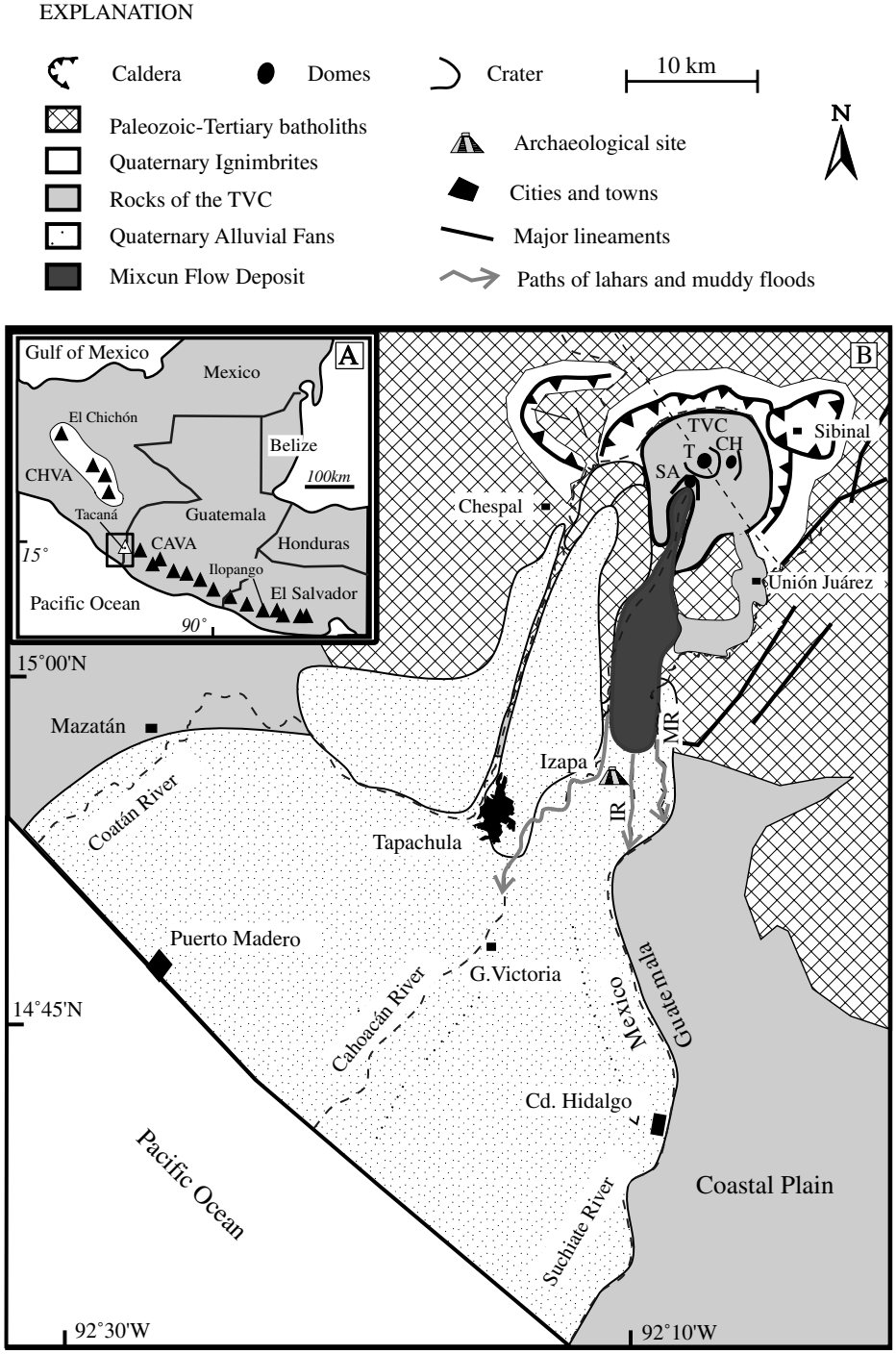

Figure 1. (A) General location of the Tacaná volcanic complex (TVC) on the Guatemala-Mexico border. Abbreviations: CHVA—Chiapanecan volcanic arc, CAVA—Central America volcanic arc, CH—Chichuj, T—Tacaná, and SA—San Antonio. (B) Simplified geological map of the TVC that shows its location within a major caldera depression. The distribution of the Mixcun flow deposit is shown in a dark gray pattern bounded by the Cahoacán and Mixcun Rivers. Collapse contours mark major collapse structures observed in air photographs and satellite imagery as well as field reconnaissance. The alluvial fans consist of fluviatile, laharic, and lacustrine deposits derived from the TVC. IR—Izapa River and MR—Mixcun River.

Figure 2. Panoramic view to the north of the Tacaná volcanic complex, from right to left: Chichuj (3800 m), Tacaná (4060 m), and San Antonio volcano (3700 m, marked with an arrow).

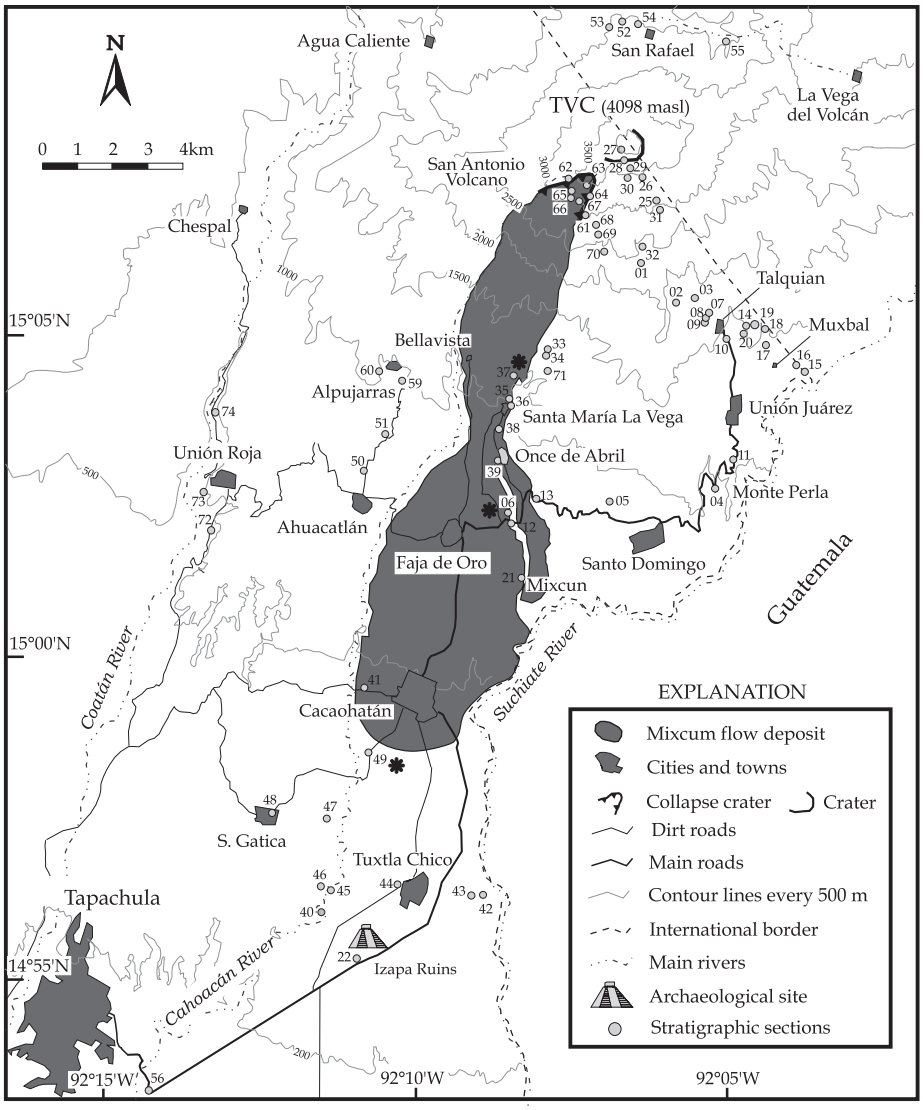

Figure 3. Simplified topographic map of the Tacaná volcanic complex (contour interval = 100 m). Map is compiled from topographic maps (scale 1:50 000 of Instituto Nacional de Estadística, Geografía e Informática, Mexico, and Instituto Geográfico Militar, Guatemala) and shows the location of selected stratigraphic sections of the Mixcun flow deposit and other related sites. Asterisks represent the sites of sedimentological analyses of Figure 7.

dome is a younger smaller andesite dome that makes up the highest peak of the volcano and represents the last activity at Tacaná. The summit of the San Antonio volcano is relatively flat, with only minor relict protrusions, and is capped by a scar or flank failure structure to the southwest. Small dacitic lava flows extend in a south-southeast direction outward from the summit of San Antonio volcano.

The Mixcun flow deposit crops out from San Antonio's summit extending south-southwest for about 14 km between the Cahoacán and Mixcun Rivers, which drain to the Suchiate River and finally to the Pacific Ocean (Fig. 1B). In proximal areas, around such communities as Santa María la Vega and Once de Abril, the deposit is confined within a narrow valley restricted by a flank failure escarpment of San Antonio volcano. Beyond this valley, around Mixcun, the deposit spreads out into a nearly flat plain extending distally to the towns of Tuxtla Chico and Cacaohatán (Fig. 1B).

STRATIGRAPHIC RELATIONS AND AGE OF THE DEPOSIT

Figure 3 shows the sites where we carried out detailed analyses of the deposit; selected stratigraphic columns from those sites are shown in Figure 4. In the Cahoacán valley, the Mixcun flow deposit overlies an older block and ash-flow deposit in some places, or a gray andesitic lava (belonging to the main edifice of Tacaná volcano) in others (site 69, Fig. 3). On the outskirts of Santa María la Vega the deposit covers a brown ash flow dated at about 10 000 yr B.P. (site 37, Fig. 4; see Table 1, samples 37b and 37c). In other localities the Mixcun flow deposit directly overlies the granitic Tertiary basement.

At site 37 the Mixcun flow deposit is overlain by a dark brown paleosol of silty sand containing

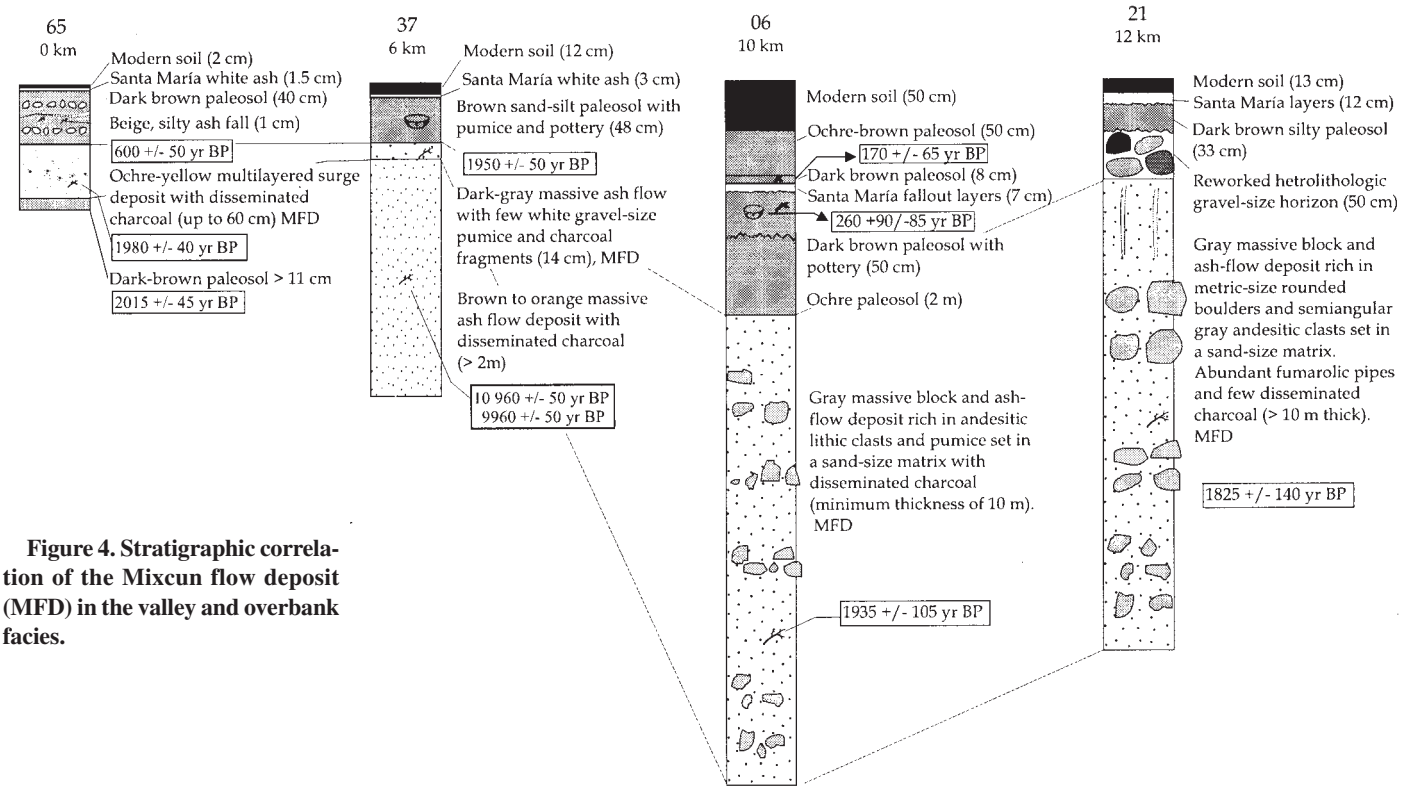

Figure 4. Stratigraphic correlation of the Mixcun flow deposit (MFD) in the valley and overbank facies.

rounded white pumice, abundant charcoal, and pottery (Fig. 4). Charcoal dated at this site yielded an age of 140 ± 50 yr B.P. (sample 37e). At other sites, the age of this paleosol ranges from 105 to 110 yr B.P. (see Table 1, samples 10 and 16). This soil horizon is overlain in all sections by fallout from the 1902 eruption of the nearby Santa María volcano in Guatemala (Rose, 1972; Williams and Self, 1983). This tephra consists of two green and whitish layers of fine sand, which are capped by the modern soil (Fig. 5). Although charcoal was present in most outcrops of the Mixcun flow deposit, typically only minute amounts were found, limiting us to accelerator mass spectrometry (AMS) analyses (37d, 12, 21, 65c, Fig. 3). The three samples of the charcoal dated by the AMS method yielded ages of 1950 ± 50, 1935 ± 105, and 1825 ± 140 yr B.P. (Table 1).

TABLE 1. RADIOCARBON DATES OBTAINED FOR THE MIXCUN PYROCLASTIC FLOW AND ASSOCIATED PYROCLASTIC DEPOSITS AND PALEOSOILS

Sample number	Location		Sample type	Conventional age (yr B.P.)	Calibrated age	Calibrated age range (± 1σ)	Observations
	lat North	long West					
37b†	15°03′51″	92°08′29″	Charcoal	10960 ± 50	11035, 12984 B.C.	11169–10948, 11205–10879, 10778–10707 B.C.	Ash-flow deposit
37c†	15°03′51″	92°08′29″	Charcoal	9960 ± 50	9385, 9372, 9349, 9320, 9313 B.C.	9599–9557; 9460–9439;9394–9306; 9297–9292 B.C.	Ash-flow deposit
65d§	15°07′28″	92°07′09″	Paleosol	2015 ± 45	N.A.	N.A.	Paleosol on top of San Antonio Volcano
38§	15°07′28″	92°07′09″	Charcoal	2370 +280/-203	401 B.C	799–165 B.C.	MFD
65c*†	15°07′28″	92°07′09″	Charcoal	1980 ± 40	A.D. 25, 43, 47	2 B.C.–A.D. 76; 46 B.C.–A.D. 121	Charcoal in surge deposit on top of San Antonio V.
37d*†	15°03′51″	92°08′29″	Charcoal	1950 ± 50	A.D. 34, 36, 61	A.D. 2–187; 101–123	MFD
12*†	15°02′16″	92°08′36″	Charcoal	1935 ± 105	A.D. 72	43–6 B.C.; 5 B.C.–A.D. 183	MFD
21*†	15°01′12″	92°08′19″	Charcoal	1825 ± 140	A.D. 219	A.D. 30–40; 51–385	MFD
65b	15°07′28″	92°07′09″	Charcoal	600 ± 50	A.D. 1327, 1346, 1393	A.D. 1300–1372; 1378–1406	Charcoal in paleosol
29§	15°07′41″	92°06′23″	Charcoal	185 ± 65	A.D. 1676, 1774, 1800, 1942, 1954	A.D. 1657–1702; 1718–1819; 1858–1861; 1917–1954	Below Santa María Ash
37e†	15°03′51″	92°08′29″	Charcoal	140 ± 50	A.D. 1685, 1732, 1808, 1926, 1948	A.D. 1670–1780; 1798–1891; 1908–1950	Below Santa María Ash
10†	15°04′51″	92°04′56″	Paleosol	110 ± 50	N.A.	N.A.	Below Santa María Ash
16§	15°05′03″	92°04′35″	Paleosol	105 ± 40	N.A.	N.A.	Below Santa María Ash

Notes: N.A.-not analyzed; MFD—Mixcun flow deposit.
*Samples analyzed by the accelerator mass spectrometry (AMS) method.
†^{14}C samples analyzed at the U.S. Geological Survey Laboratory, [location], by J. McGeehin.
^{14}C samples analyzed at Isotope Geochemistry Laboratory of the University of Arizona by A. Long and C. Eastoe.

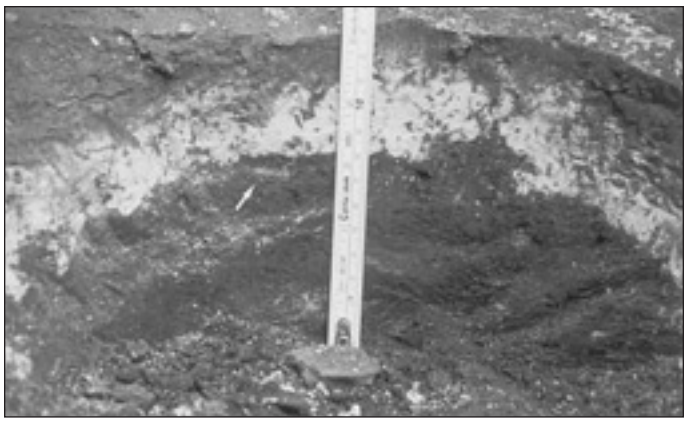

Figure 5. Paleosol with pottery fragments on top of the Mixcun flow deposit and underlying the 1902 ash from Santa María Volcano, Guatemala.

Figure 6. Channel facies exposure of the Mixcun flow deposit as seen at section 21 close to the Mixcun town. At least two flow units can be recognized from alignments of lithics.

Only at a locality near Once de Abril (38, Fig. 3) did abundance and size of the fragments permit age determination by standard ^{14}C techniques ($2370\ ^{+280}/_{-203}$ yr B.P., Table 1).

At the northern edge of San Antonio volcano's summit (section 65, Figs. 3 and 4) the deposit correlates with a 30-cm-thick multilayered surge deposit dated with the AMS method at 1980 ± 40 yr B.P. (sample 65c). Here, the Mixcun flow deposit surge overlies a dark brown paleosol (>5 cm) dated at 2015 ± 45 yr B.P. (sample 65d). The sequence continues with a dark brown paleosol (35 cm thick) dated as 600 ± 50 yr B.P. (sample 65b) that contains two discontinuous horizons of pumice fallout, and a thin surge. The 1902 Santa Maria fall and the modern soil cap the section. Considering the AMS age of the surge deposit and that of the paleosol it seems likely that the surge layers represent the beginning of the San Antonio eruption and that they were preserved after the major explosion in the northern part of the summit. Because of the closeness of the four AMS dates, which were obtained from different sites by different laboratories, it is probable that three ages (12, 37d, and 65c) are closer to the true age of the deposit. An approximate age of 1950 yr B.P. is used in the remainder of this paper. Calibration of these sample ages (Stuiver and Reimer, 1986) yielded calendar ages between A.D. 25 and 72 (range ± 1σ, 38 B.C.–A.D. 216, see Table 1).

Internal Stratigraphy, Sedimentology, and Components

The stratigraphy of the Mixcun flow deposit varies from sites located within main gullies (channel facies) and from sites located in the valley walls (overbank facies) and are described accordingly.

Channel Facies. The deposit is a light gray, massive, matrix-supported unit. It is composed of dispersed gray andesitic and accidental red andesite lithic clasts of gravel to boulder size set in a coarse sand- to silt-size matrix (Figs. 3 and 5). In many outcrops the Mixcun flow deposit consists of two or three flow units, each with a weak alignment of inversely graded lithic clasts (Fig. 6). Some outcrops exhibit fumarolic pipes several decimeters to a meter long, enriched in gravel-size clasts and disseminated charcoal. At section 21, the deposit is enriched in subrounded accidental boulder-size clasts, giving the deposit a laharic appearance. The upper parts of the deposit are partly altered to a light brown paleosol.

The grain size of the channel facies is summarized in Figure 7A. At locality 6, the deposit is 9 m thick and consists of two flow units, each with an inversely graded basal layer ~20 cm thick. For granulometric analyses, the section was subdivided into six layers, each 1.5 m thick. Fine sediment (<16 mm, –4ϕ) was sampled directly in the field using channel sampling methods and grain-size distribution was determined by dry sieving down to 0.063 mm (4ϕ). The distribution of clasts greater than –4ϕ was determined by point-counting in photographs. The grain-size distribution within the Mixcun flow deposit is consistent, with medians for the sampled layers between 8 to 12.99 mm (–3.0 to –3.7ϕ), sorting of 3.5 to 3.9ϕ, and skewness of +0.50 to +0.56. The histograms are bimodal with modes in the 32–64 mm (–5.0 to –6.0ϕ) range (associated with the matrix-supported clasts) and the 0.125–0.25 mm (2.0–3.0ϕ) range (the matrix of the deposit).

The coarser lithological components of the Mixcun flow deposit were identified visually in the field by naked eye. The components finer than 8 mm (3.0ϕ) were identified with a binocular microscope. Clasts coarser than 1 mm (0ϕ) were subdivided into andesite (light gray, dense, dark gray, and glassy), banded andesite, accidental red andesite (altered red andesites from the old edifice), and free crystals (commonly plagioclase). Clasts finer than 0ϕ were grouped into either juvenile (juvenile material including glass) or free crystals (Fig. 7A). Among the matrix-supported clasts, andesites are most common (38–100 wt%), the banded andesites account for 20–50 wt%, and the altered red andesites are the least common (6–25 wt%) component. In the matrix, the free crystal component increases (15–99 wt%) with decreasing grain size at the expense of the juvenile component (1–85 wt%). This increase in the amount of crystals in the deposit may be related to grain size but may also be related to density-controlled sorting processes. The dense crystals may have been concentrated in the matrix while the less dense glassy material may have been lost to the elutriated ash cloud.

Overbank Facies. The Mixcun flow deposit is also exposed on the outskirts of Santa María la Vega on the margins of the Mixcun gully (section 37, Fig. 4). In these outcrops the deposit is a light gray, massive unit with abundant charcoal. The deposit has a maximum thickness of 1 m and pinches out laterally away from the axis of the channel. The unit consists of gravel-size altered pumice embedded in a homogeneous sand-size matrix. A 5-cm-thick inversely graded layer that lacks matrix-supported clasts occurs at its base. It consists of silty sand with a mean of 0.57 mm (0.8ϕ) and sorting of 2.2ϕ. The overlying bulk of the unit is 1 m thick and includes matrix-supported clasts <64 mm (–6ϕ) in diameter (Fig. 7B). The majority of the overbank outcrops show matrix-supported clasts that are finer grained than in the channel facies and have a

lower overall mean grain size (–1.4ϕ). The proportions of the different components in the overbank deposit are similar to those found in the channel deposits.

Secondary Deposits. Several outcrops beyond the distal extent of the Mixcun flow deposit expose a complex sequence of debris flow and hyperconcentrated flow deposits. At locality 49, about 0.5 km south of the distal edge of the Mixcun flow deposit, a series of massive sand to silt beds (lenses 0.5–3 m thick) are present. They contain minor amounts of matrix-supported gravel-size clasts and are interbedded with low-angle (10º–35°) cross-stratified beds (0.5–2 m thick). Figure 7B shows the grain-size distribution of one of the massive beds at this locality. The massive units have means of 0.35 to 0.57 mm (1.5 to 0.8ϕ) with a sorting between 3.0 and 3.5ϕ. The cross-stratified hyperconcentrated flow deposits consist of a series of fine (mean 0.46–4.29 mm [1.1 to –2.1ϕ]; sorting 1.0–1.5ϕ) and coarse-grained laminations (with means of 0.81–13.93 mm [0.3 to –3.8ϕ] and sorting of 1.6–2.3ϕ) defining what appear to be antidune type bedforms.

The components of these secondary beds at this locality are fundamentally the same as that of the Mixcun flow deposit; however, they show lesser amounts of the red andesites of the old edifice (3–11 wt%). The most extensive outcrop of the debris flow and hyperconcentrated flow deposits is found in the bank of the Cahoacán River in the outskirts of Tapachula (site 56, Fig. 8). Here, a 10-m-thick sequence comprises seven matrix-supported units consisting of gravel-size gray andesite, with subrounded lithics and pumice contained in a medium sand matrix. These units show typical dewatering forms such as dish structures and low-angle cross-stratification that are typical of hyperconcentrated flow deposits (Scott et al., 1995). One of the intermediate units shows an excellent transverse section from channel to marginal facies where the materials vary from debris to hyperconcentrated flow deposits (Fig. 8).

VOLUME ESTIMATE

The Mixcun flow deposit covers an area of at least 25 km^2. In most of the exposures the deposit varies in thickness from 1 to more than 10 m. If we consider an average present thickness of 5 m for the Mixcun flow deposit, a minimum volume of 0.12 km^3 is calculated. This value is a minimum because it does not include deposits lost to erosion. The Mixcun flow deposit is considerably larger than similar deposits produced by recent Merapi-type eruptions associated with partial dome collapse (e.g., Merapi, Indonesia, 1984; Colima, Mexico, 1991; Unzen,

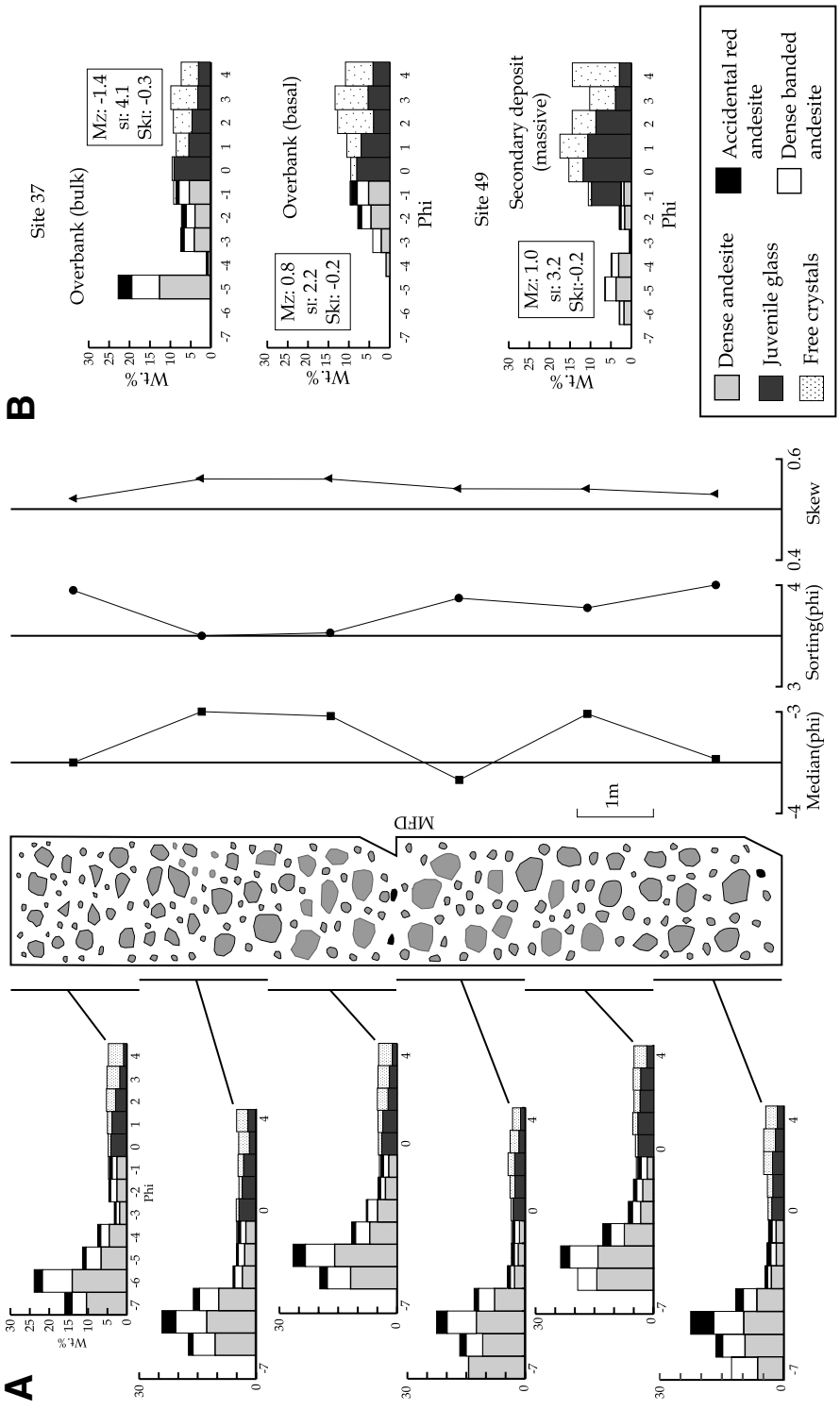

Figure 7. (A) Variation of grain size, mean, sorting, and skewness (using methods of Folk and Ward, 1957), and components through the Mixcun flow deposit at locality 6. (B) Grain-size histograms and components of the overbank (locality 37) and secondary (locality 49) deposits associated with the Mixcun flow deposit.

Figure 8. View of a series of debris and hyperconcentrated flow deposits exposed at locality 56 along the Cahoacán River at the outskirts of the city of Tapachula. In the debris-flow facies, the lower third of the deposit shows an alignment of lithics that disappears toward the marginal deposit facies (arrow).

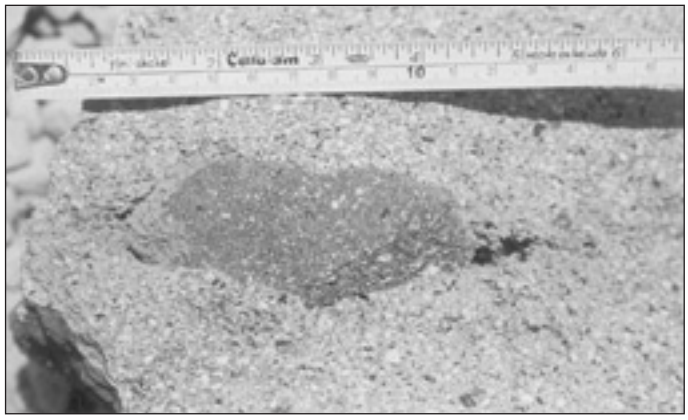

Figure 9. Detail of a basaltic andesite enclave hosted by an evolved andesite as found at section 21. Note the margins of the enclave in contact with host rock.

Japan, 1990–1995; Soufrière Hills, Montserrat, West Indies, 1992–1997) (Table 2). In fact, it is similar to the volume of the basal avalanche deposit of the 1902 eruption of Mount Pelée, Martinique (Bourdier et al., 1989). The Mixcun flow deposit volume coupled with the shape of the escarpment at the San Antonio volcano and the dispersion of the pyroclastic flow deposit, suggest a Peléan-style eruption.

PETROGRAPHY AND MINERAL CHEMISTRY OF MIXCUN FLOW DEPOSIT

Modal abundances of five juvenile Mixcun flow deposit samples were analyzed by counting between 600 and 1000 points (Table 3). The dense clasts (21dl and 21dlmi) are hypocrystalline, porphyritic, and can be classified as two-pyroxene hornblende andesites. Their mineral assemblage is dominated by euhedral to subhedral phenocrysts of plagioclase > hornblende > enstatite > augite > accessory phases (apatite and titanomagnetite) embedded in a glassy cryptocrystalline groundmass. Samples 20mi and 21dlmi are classified as olivine-bearing two-pyroxene basaltic andesites (hereafter mafic inclusions; see Fig. 9) that consist of plagioclase > hornblende >

TABLE 2. IMPORTANT HISTORIC AND MODERN VOLCANIC ERUPTIONS RELATED TO THE PARTIAL OR TOTAL DESTRUCTION OF DOMES AND LAVA FLOWS AND THEIR COMPARISON WITH THE TACANÁ ERUPTION OF 1950 YR B.P.

Volcanic event	Date (yr A.D.)	Eruption type	Brief description of deposits	Volume (km^3)	References
Santiaguito, Guatemala	1976–1977	Merapi	Nuée Ardente (block and ash-flow and surge deposits) from the distal end of a blocky dacite lava flow	2×10^{-5}	Rose et al. (1976–1977)
Merapi, Indonesia	1984	Merapi	Four nuées ardentes produced from the destruction of viscous lava domes	4.5×10^{-3}	Boudon et al. (1993)
Colima, Mexico	1991	Merapi	Block and ash-flows and ash clouds from partial dome collapse	8×10^{-4} and 2×10^{-2}, respectively	Rodríguez-Elizarrarás et al. (1991)
Unzen, Japan	1990–1995	Merapi	Hundreds of block and ash flows from partial dome collapse	From 1×10^{-4} to 1×10^{-6}	Matsuwo et al. (1997)
Soufrière Hills, Monserrat	1992–1997	Merapi	Small runout pyroclastic flows (<1 km); large runout pyroclastic flows (as large as 6.5 km)	2×10^{-2} DRE, $1–9 \times 10^{-3}$ DRE	Cole et al. (1998)
Mount Pelée, Martinique	1902	Pelée	High-aspect-ratio ignimbrite from a lateral explosion	$1–1.5 \times 10^{-2}$	Bourdier et al. (1989)
Tacaná, Mexico	1950 yr B.P.	Pelée	Series of block and ash flows from a lateral explosion	12×10^{-2}	
Mayon, Philippines	1968	Soufrière	Nuées ardentes fed by fallback from ~600-m-high column	15×10^{-3}	Moore and Melson (1969)
Ngauruhoe, New Zealand	1975	Soufrière	Pyroclastic avalanches produced by the collapse of the dense column interior, individual avalanches did not have a volume larger than $10^3–10^6$ m^3	$1–1.5 \times 10^{-3}$, $0.6–0.9 \times 10^{-3}$ DRE	Nairn and Self (1978)
Chichón, Mexico	1982	Soufrière—hydromagmatic	Two block and ash flows and pyroclastic surges fed from a fountain of pyroclasts	5×10^{-7}	Macías et al. (1998)
Mount St. Helens, USA	1986	Gravitational collapse or explosion	Basal avalanche (block and ash flow) followed by a pyroclastic flow, and ash-cloud surge	5×10^{-4}, 3×10^{-5}, and 6×10^{-6}, respectively	Mellors et al. (1988)
Cerro Quemado Dome Complex, Guatemala	4 ka	Merapi	Pyroclastic flow deposit (Qcq3pfa) associated with an edifice collapse occurred ca. 1150 yr B.P.	3.1×10^{-2}	Conway et al. (1992)

Note: DRE—dense rock equivalent.

TABLE 3. PETROGRAPHY OF SELECTED SAMPLES OF THE MIXCUN FLOW DEPOSIT

Sample number		20mi Basaltic andesite	21dl Andesite	21dlmi Andesite	21gl Andesite	64lf Dacite	66lf Dacite
Qz	Ph	0.0	0.0	0.0	0.0	2.1	0.52
	Mph	0.0	0.0	0.0	0.0	0.0	2.79
K-Feld	Ph	0.0	0.0	0.0	0.0	2.1	0.52
	Mph	0.0	0.0	0.0	0.0	6.5	1.86
Plag	Ph	2.2	13.28	11.30	12.67	12.1	12.18
	Mph	33.1	9.57	8.05	7.23	8	11.26
Hbd	Ph	1.4	3.10	2.60	3.50	1.1	0.10
	Mph	14.7	4.00	5.10	4.00	1	0.10
Cpx	Ph	0.0	0.24	0.15	0.29	1.1	0.52
	Mph	1.3	1.17	0.15	0.39	1.5	0.83
Opx	Ph	0.3	0.68	0.15	0.29	1.2	0.41
	Mph	0.7	0.87	0.15	0.49	0.9	0.83
Ox	Ph	0.0	0.09	0.31	0.30	0.0	0.10
	Mph	4.1	2.19	2.30	2.30	2.6	0.62
Ol	Ph	0.0	0.0	0.0	0.0	0.0	0.0
	Mph	0.8	0.0	0.0	0.0	0.0	0.0
Vesicles	N.A.	7.8	3.00	11.6	2.57	2.7	1.65
mi	N.A.	0.0	0.0	0.0	0.0	0.0	0.63
Matrix	N.A.	33.6	61.6	57.9	65.25	57.3	65.12
Total	N.A.	100.00	100.00	100.00	100.00	100.00	100.00

Note: The modal analysis (vol%) includes 600–1000 counted points. Abbreviations: mi—mafic inclusion, dl—dense lithic, gl—glassy lithic, lf—lava flow, d—dome, Qz—Quartz, K-Feld—Anorthoclase, Plag—Plagioclase, Hbd—Hornblende, Cpx—Clinopyroxene, Opx—Orthopyroxene, Ox—Oxides, and Ol—Olivine, Ph—Phenocrysts (>0.5mm), and Mph—Microphenocrysts (>0.05mm, <0.5mm) (after Francalanci, 1987). N.A.—not analyzed.

enstatite > augite > olivine and accessory apatite and titanomagnetite. They have an intergranular texture in which the void spaces between the Ca-rich plagioclases are occupied by hornblende, pyroxenes, oxides, and traces of olivine.

The dacites (66lf) consist of plagioclase > K-feldspar > quartz > pyroxene > hornblende, and minor titanomagnetite embedded in a glassy groundmass with abundant microphenocrysts and rare vesicles. The rock has a pilotaxitic texture with phenocrysts of plagioclase (sieve and spongy textures) and minor pyroxenes, and microphenocrysts of all mineral phases.

The plagioclase phenocrysts and microphenocrysts (19%–35%) in the dense andesitic lithic clasts have normal and reverse zoning and abundant glass and fluid inclusions that give the crystals sieve and spongy textures. Several crystals have been resorbed and others show a sheared texture. The composition of zoned plagioclase phenocrysts varies from $An_{50–70}$ (core) to $An_{42–82}$ (rim), whereas plagioclase in the mafic inclusions varies from $An_{67–81}$ (core) to $An_{62–76}$ (rim) (Fig. 10).

Hornblende is present as phenocrysts and microphenocrysts in the dense lithics (8%) and in the mafic inclusions (14.7%), where it shows a sheared texture and reaction rims. In general, hornblende crystals are highly fractured, with inclusions of titanomagnetite, apatite, and plagioclase.

The clinopyroxenes and orthopyroxenes are also present as phenocrysts and microphenocrysts (1.5%) in the dense lithics, and only as microphenocrysts in the mafic inclusions (0.6%–1.6%). In both cases they have subhedral to anhedral forms with sheared texture, reaction rims, and normal zoning. Chemically they do not show major variations in composition, varying only from En_{43} to En_{49} in both types of rocks. Olivine is present as microphenocrysts and traces in the mafic inclusions and has a very constant composition, of $Fo_{76–79}$.

The groundmass of the dense lithics is composed of dark and light brown banded glass with cryptocrystals and semicircular vesicles. The glass composition in the groundmass varies widely from 63 to 76 wt% SiO_2. In contrast, the groundmass composition of the mafic inclusions is more homogeneous, with a rhyolitic composition (73–74 wt% SiO_2).

WHOLE-ROCK CHEMICAL ANALYSES

Major, trace, and rare earth elements were determined for eight juvenile samples of the Mixcun flow deposit (Table 4). These analyses indicate that the Mixcun flow deposit rocks belong to the subalkaline series and fall into the calc-alkaline field of continental volcanic arcs (Irvine and Baragar, 1971). In the SiO_2 versus K_2O diagram (Fig. 11A), the rocks plot in the K-medium field of the calc-alkaline suite (Gill, 1981) varying from basaltic andesite (53.86% SiO_2) to dacite (64.41% SiO_2).

The basaltic andesite (mafic inclusion) is only enriched in MgO, CaO, TiO_2, Cr, and depleted in K_2O, Rb, Y, and Zr relative to the andesites and dacites. The dacites (64d and 66lf) have stronger enrichments in Y and Zr with respect to the andesites. This is probably due to crystallization of anorthoclase and apatite (abundant accessory phase) associated with extensive magmatic differentiation. A longer residence time for the dacitic magma is supported by the enrichment of Sr in these rocks, which also suggests contamination at shallow pressures. The andesites are characterized by enrichments of K_2O and Rb relative to the dacites, suggesting fractionation of hornblende from the andesitic magma. The andesites in the Mixcun flow deposit are enriched in the light rare earth elements (REEs) (La, Ce, and Nd) and the heavy REEs (Tb and Yb) relative to the basaltic andesite enclave. The spider diagram shows the andesites consistently having larger abundances of all elements than the basaltic andesite enclave, with the exception of Sr and Ta (Fig. 11B).

DISCUSSION

Magma Mixing as the Triggering Process of the 1950 yr B.P. Eruption

Around 1950 yr ago, volcanic activity within the Tacaná volcanic complex moved to the San Antonio volcano, the crater of which was filled at the time by an andesitic dome. As the chemical composition of the dense lithics and pumice within the Mixcun flow deposit are very similar, we speculate that prior to the eruption the andesitic summit dome (similar to the present dome) capped the top of a column of magma of similar chemical composition. There are several lines of evidence suggesting that the 1950 yr old eruption was triggered by intrusion of a hot, volatile-rich mafic magma into a colder reservoir filled with a homogeneous crystalline andesitic melt. The mafic melt is represented by <5% olivine-bearing basaltic andesite inclusions (54% SiO_2) that mingled with the andesite host melt (60%–63% SiO_2) represented by dense, glassy, and banded lithic clasts. These andesite lithic clasts have plagioclase phenocrysts with sieve, spongy, and sheared textures, normal and inversely zoned reaction rims, and heterogeneous groundmass glass compositions (63%–76% SiO_2). In contrast, the mafic inclusions have normally zoned phenocrysts of plagioclase, a stable glass groundmass composition, enrichments in MgO, CaO, Ni, and Cr, and incompatible element concentrations typical of poorly differentiated magmas. As the mafic inclusions are in sharp contact with the andesite host rock, and some of their minerals (e.g., olivine, plagioclase) have a stable core-rim chemical composition, we interpret both features as quenched structures

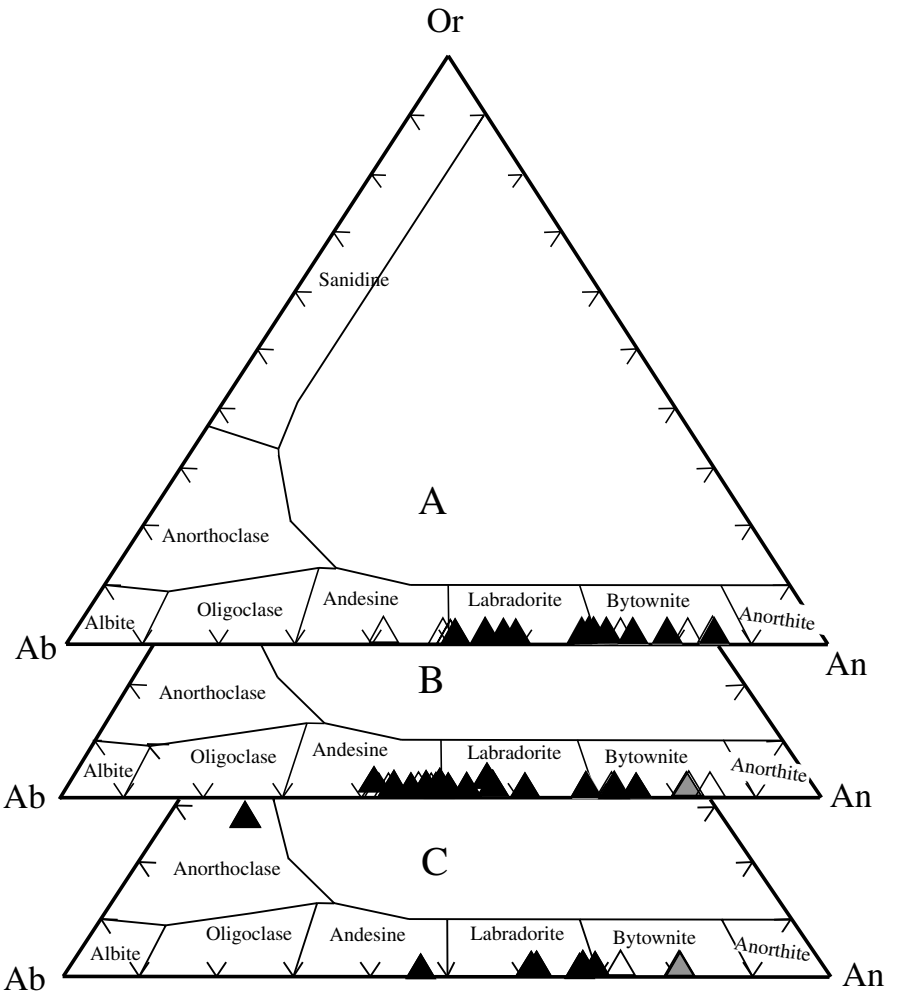

Figure 10. Chemical composition of plagioclase phenocrysts, microphenocrysts, and microcrystals of mafic inclusions (A), dense andesites (B), and dacites (C). Triangles: filled—core, empty—rim, and gray—microcrystals in orthopyroxene in samples B and C.

(Bacon, 1986; Bacon and Metz, 1984; Blundy and Sparks, 1992; Eichelberg, 1980; Heiken and Eichelberg, 1980; Koyaguchi, 1986). The andesites of the Mixcun flow deposit have several disequilibrium characteristics that have been cited as typical features of magma-mixing processes, such as spongy, sieve, and cellular textures of plagioclase phenocrysts (Eichelberg, 1978; Koyaguchi, 1986; Sakuyama, 1984), glass inclusions in plagioclase (Halsor, 1989), and variable groundmass glass compositions. Other authors have considered basaltic, basaltic andesite, and andesite inclusions (Murphy et al., 1998; Seymour and Vlassopoulos, 1992) embedded within more evolved host rocks as the mafic end member of explosive eruptions caused by magma mixing. Therefore, we propose that an intrusion of a hot basaltic andesitic melt into a cooler crystalline andesitic reservoir caused superheating of the andesitic magma and quenching of the basaltic andesite. Because the Mixcun flow deposit does not contain products of intermediate composition, we suggest that mixing between both magmas had a short duration. The mafic melt was rapidly quenched and disrupted into liquid drops that then partially reacted with the cooler andesite host until they solidified (Koyaguchi, 1986). This mixing process was too brief to cause convection and homogenization of the two liquids as observed in some experimental studies (Kouchi and Sunagawa, 1985). Instead, it is likely that sudden crystallization of the mafic magma resulted in vesiculation that triggered an explosive eruption.

Laterally Driven Explosion of San Antonio Volcano

We suggest that overpressure in the magmatic system due to vesiculation promoted phreatic-phreatomagmatic explosions at the summit dome that in turn generated short runout surge clouds hot enough to burn vegetation on their paths. These explosions caused destabilization of the weakest zone of the San Antonio volcanic edifice and resulted in a laterally driven Peléan-style eruption. Subsequently partial collapse of the south-southwest portion of the San Antonio dome produced a laterally driven explosion over a 30° sector. The disintegration of the summit dome generated a series of pyroclastic flows (block and ash flows). Proximally, the Mixcun pyroclastic flows were funneled along the narrow Cahoacán valley where they flowed down steep slopes (20°–30°) and eroded the substrate. The pyroclastic flows overtopped small tributaries, filling channels in the main valley, and overflowed their margins to the present area of Santa María la Vega, 7 km from the summit. In this area, the Cahoacán valley rapidly narrows to a deep gorge that then broadens to a wide fan with an average slope of 5°. In the gorge the pyroclastic flows were highly erosive, but beyond the valley mouth they lost velocity and their capacity to transport large boulders. This area of flow transition was characterized by intense sedimentation, as indicated by the thick exposures (10–15 m) near Once de Abril and Mixcun. We are uncertain of the maximum extent of the pyroclastic flows because the thick vegetation cover obscures their recognition beyond the neighborhood of Cacaohatán. Syneruptive and secondary debris and hyperconcentrated flows were derived from the primary pyroclastic flows, probably from intense rain and spring discharges. These flows followed the Cahoacán and Mixcun Rivers, inundating areas close to Tapachula and the pre-Hispanic center of Izapa, and they most likely continued to the Pacific Ocean. The eruption ended with the emission of viscous andesitic and dacitic lava flows from the summit of San Antonio volcano, creating its present morphology.

Archaeological Implications: Past Hazards

The Tacaná volcanic complex is located at the southern edge of the so-called Soconusco region that extends along the Chiapas coastal plain for about 240 km from the town of Pijijiapan in the north to beyond the Mexico-Guatemala border (Voorhies, 1989) (Fig. 12). The first known record of occupation in the area dates back to the Archaic period, ca. 7500 yr B.P. (Voorhies, 2000) by the Chantuto people. These settlers, who led a sedentary life style without production of pottery, exploited the coastal lagoons and estuaries of Soconusco (Michaels and Voorhies, 1999). Production of pottery in the region started some time af-

TABLE 4. WHOLE-ROCK CHEMICAL ANALYSES OF SELECTED SAMPLES FROM THE MIXCUN FLOW DEPOSIT

Sample	TAC9320dl*	TAC9721dl*	TAC9721gl*	TAC9721p*	TAC9721mi*	TAC9864d†	TAC9866lf†	TAC9867lf†
SiO_2	61.98	61.77	61.24	60.36	53.85	64.41	64.21	61.90
Al_2O_3	16.70	16.83	16.94	16.47	18.23	17.03	17.58	17.79
Fe_2O_3	5.71	5.84	6.11	5.82	8.65	3.57	3.71	4.44
MnO	0.10	0.10	0.11	0.10	0.13	0.09	0.08	0.01
MgO	2.30	2.36	2.45	2.23	4.07	2.31	1.71	2.81
CaO	5.64	5.67	5.74	5.52	8.40	5.04	4.94	5.96
Na_2O	3.80	3.79	3.77	3.68	3.52	3.82	4.64	3.71
K_2O	2.34	2.20	2.17	2.18	1.31	2.17	1.85	2.05
TiO_2	0.56	0.58	0.59	0.56	0.88	0.45	0.48	0.55
P_2O_5	0.14	0.15	0.15	0.15	0.15	0.15	0.10	0.12
LOI	0.45	0.32	0.41	2.46	0.57	0.59	0.56	0.39
Total	99.73	99.61	99.67	99.53	99.77	99.99	100.00	100.00
Sr	481	483	490	471	468	477	638	481
Ba	699	722	677	669	490	428	894	765
Co	13.1	13.7	13.7	14.5	23.5	N.D.	N.D.	N.D.
Cr	15.2	15.1	12.9	11.3	34.0	2	10	6
Cu	14.0	15.0	14.0	15.0	26.0	N.D.	N.D.	N.D.
Ni	5.0	6.0	4.0	6.0	11.0	N.D.	N.D.	N.D.
Sc	10.1	11.1	10.2	10.2	21.2	N.D.	N.D.	N.D.
Th	4.1	4.2	3.8	4.3	2.0	N.D.	N.D.	N.D.
Pb	14.0	20.0	15.0	13.0	6.0	N.D.	N.D.	N.D.
V	105	109	112	107	211	N.D.	N.D.	N.D.
Zn	76.0	78.0	83.0	77.0	92.0	N.D.	N.D.	N.D.
Y	15	15	15	15	16	19	17	19
Rb	61	68	58	64	29	47	50	57
Zr	122	122	126	116	95	146	154	144
Be	2	2	2	2	2	N.D.	N.D.	N.D.
Cs	2.5	2.5	2.3	2.5	1.3	N.D.	N.D.	N.D.
Hf	3.7	3.7	3.4	3.6	2.5	N.D.	N.D.	N.D.
Ta	<0.3	<0.3	<0.3	<0.3	<0.3	N.D.	N.D.	N.D.
U	1.3	1.3	1.3	1.4	0.6	N.D.	N.D.	N.D.
Cd	<0.5	<0.5	<0.5	<0.5	<0.5	N.D.	N.D.	N.D.
La	16.5	17.3	15.7	16.5	10.7	19	17	15
Ce	34	34	33	33	24	20	30	25
Nd	14	15	14	15	13	N.D.	N.D.	N.D.
Yb	1.41	1.51	1.42	1.44	1.46	N.D.	N.D.	N.D.
Lu	0.21	0.24	0.21	0.22	0.22	N.D.	N.D.	N.D.
Eu	0.84	0.89	0.81	0.87	0.90	N.D.	N.D.	N.D.
Sm	2.97	3.15	2.83	2.97	2.87	N.D.	N.D.	N.D.
Tb	0.4	0.5	0.4	0.4	0.4	N.D.	N.D.	N.D.

Note: Major elements (wt% on H_2O-free basis, all Fe as Fe_2O_3), trace elements (ppm), and rare earth elements (ppm). LOI—loss on ignition.

*Activation Laboratories Ltd., Ontario, Canada. Major and trace elements analyzed by ICP (inductively coupled emission spectrometry); Nd, Co, Cr, Sc, and Rb by INAA (instrumental neutron activation analysis).

†Dipartimento di Scienze della Terra, Università degli Studi di Firenze, Italia.

ter 3500 yr B.P. (i.e., 1500 B.C.; early pre-classic) associated with the rise of the Barra people (Lowe, 1977; Blake et al., 1995), although it is uncertain whether they were descendants of the Chantuto (Voorhies, 1989). The first ceremonial center in the area was established at Izapa (Lowe et al., 1982) ca. 1500 B.C. and became the cultural and political center of the Soconusco region between 400 B.C. and A.D. 450 (Voorhies, 1989). Izapa was the only center with temples, courtyards, and stele and altar monuments. The center was in use until the early post-classic period, ca. A.D. 1200 (Lowe et al., 1982).

Based on pottery, calendar inscriptions, and radiocarbon dates, Lowe et al. (1982) defined 15 cultural phases of occupation at Izapa during a time span of ~2500 yr (Fig. 13). Izapa reached its apex during the Guillen phase (ca. 300–50 B.C.), during which an amazing amount of construction and sculpture was completed. The late pre-classic at Izapa is represented by the Hato phase (ca. 50 B.C.–A.D. 100), during which a recession in the construction activity at the center occurred around the first century A.D. This construction halt marked an apparent shift in activity from the middle to the northern part of the center and by the predominance of imported vessels, apparently from Guatemala or El Salvador, relative to local pottery. Lowe et al. (1982) concluded that these facts were probably related to local and foreign events of unusual cultural-historical impact and further suggested that during this period inhabitants of Izapa conquered areas east of Soconusco. The following cultural phase, Itstapa (ca. A.D. 100–250), is noticeably barren of foreign pottery and marks a stable period in the cultural history of Izapa (Fig. 13). During the 1970s several authors (Sharer, 1974, 1978; Sheets, 1971, 1976) reported that a volcanic eruption of Ilopango caldera, El Salvador, ca. A.D. 100–200, extinguished much of the life of the pre-Hispanic center of Chalchuapa in western El Salvador (Fig. 12). Influenced by this fact and because the lower boundary for the Ilopango eruption was A.D. 100, Lowe et al. (1982) proposed that this eruption could mark the cultural stabilization between the Hato and Itstapa phases at Izapa. However, the Ilopango eruption that produced the tierra blanca tephra has been more precisely dated as ca. A.D. 260 (Sheets, 1983; Hart and Steen-McIntyre, 1983), and therefore is not related to the cultural phases at Izapa (Fig. 13).

Links Between the San Antonio Volcano Activity and Izapa Temporary Abandonment. According to Lowe et al. (1982), Izapa was centered at an optimum orographic situation between the foot of the Tacaná volcanic complex and the coastal region. Its unique ecological location made Izapa a suitable place for cacao plantations and, as cacao production was the primary activity in the region, Izapa eventually became a hub of cultural influence in the eastern part of Soconusco. The main center of the Izapa area was built on a low hill between the Cahoacán and Mixcun-Suchiate Rivers, which bound a large Quaternary fan made up of conglomerate and lahar deposits. In spite of

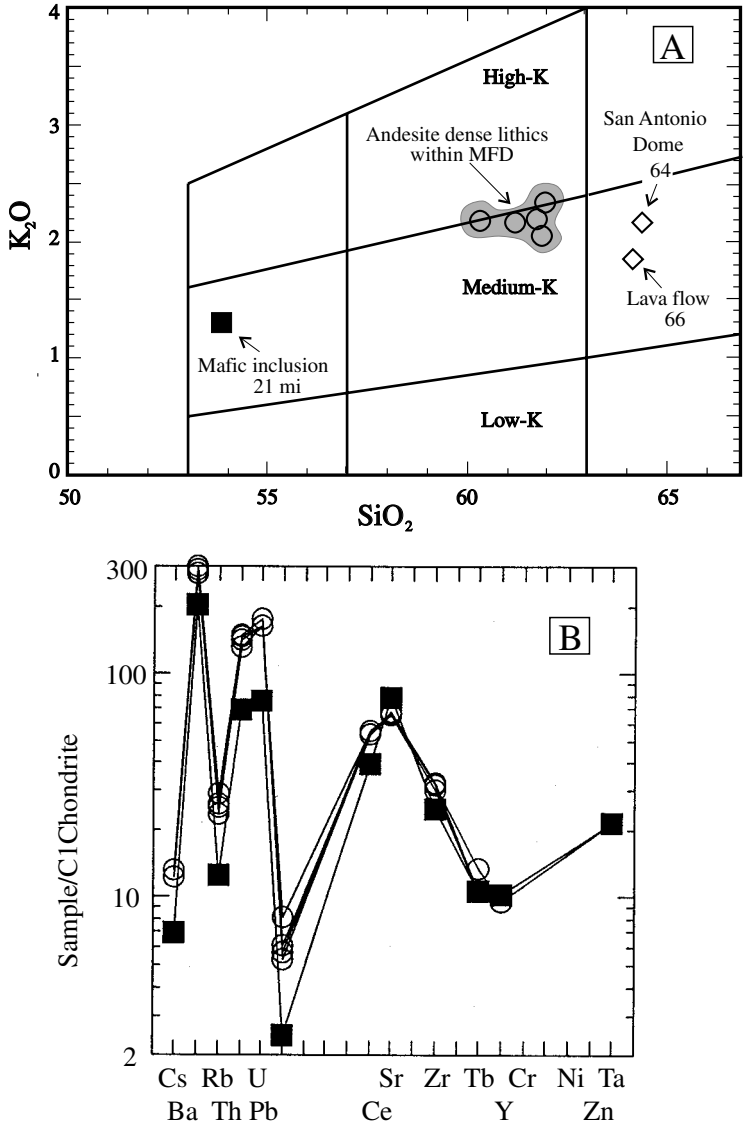

Figure 11. (A) Silica vs. potassium diagram of Gill (1981). Filled square is the mafic inclusion 21 mi, open circles are juvenile fragments within the Mixcun flow deposit and lava flow 67, and open diamonds are the dacite dome 64 and dacite lava flow 66. (B) Spider diagram of incompatible elements normalized to the primordial mantle (Wood, 1979).

its unique site, Izapa was subjected to flooding due to rainfall in the Chiapas highlands and by the volcanic activity in the Tacaná volcanic complex.

The Peléan eruption of San Antonio volcano occurred about 1950 yr B.P. (A.D. 25–72, range ±1σ, B.C. 38–A.D. 216; see Table 1), i.e., within the time span reported for the Hato phase (ca. 50 B.C.–A.D. 100) by Lowe et al. (1982). We therefore propose that this eruption was the main reason for the halt of construction activity. Deposit distributions show that pyroclastic flows from San Antonio did not directly affect Izapa; however, ash derived from overriding ash clouds could have reached the ceremonial center. Pyroclastic flow deposits filled the main valleys (Cahoacán and Mixcun) and blocked the drainage network of the area. The reestablishment of water flow during and after the event produced secondary muddy floods that followed the course of the rivers and small tributaries (e.g., Izapa) toward the distal areas and possibly as far as the Pacific Ocean. Several outcrops of debris flows and hyperconcentrated flow deposits related to the eruption occur along these channels.

We hypothesize that muddy floods following the eruption of San Antonio destroyed plantations and probably inundated parts of Izapa. Villagers fled because of the direct impact of these events or the resulting famine. In the aftermath of the eruption, Izapa was in virtual isolation with respect to other cultural centers in the area. It must have taken several years before the Izapans repopulated the area, many having migrated into Central America.

Flooding is common in the Soconusco region. During an archaeological survey along several rivers, Voorhies and Kennett (1995) discovered 22 buried sites, most of which consisted of dispersed artifacts, artificial platforms, and floors embedded in fine-grained deposits that the authors concluded were related to flooding.

A modern analog of this event occurred in September 1998, when tropical storm Pauline rainfall exceeded the amount typical for a whole year and produced muddy floods along the rivers flowing toward the Pacific Ocean. These flows destroyed several sections of the federal highway connecting Chiapas with the rest of Mexico. Notwithstanding our living in an age of great technological means, inhabitants of many settlements, from small hamlets to as large a city as Tapachula, remained isolated from the rest of the country for several days. Water, not to mention food and medicines, had to be brought into the area by air or a long detour via Guatemala.

Thus, we suggest that the temporary abandonment of Izapa, which was responsible for the construction halt during the Hato phase, should be considered the probable result of the eruption of San Antonio and subsequent flooding. The local inhabitants briefly migrated toward Central America (Guatemala and El Salvador) until more favorable living conditions were reestablished at Izapa. Therefore, it is plausible that the introduction of pottery to Izapa from Guatemala and El Salvador was by people driven out by the eruption who returned later. In this light, explanations based upon conquest should be reconsidered.

It is possible that inhabitants from Izapa never lost contact with their city and it is even feasible that some stayed in the surrounding areas, as suggested by offerings found in the southern section of Izapa (group B, mound 30d, p. 139, Lowe et al., 1982). The location of those late offerings in group B is of particular interest, considering the discovery by Lowe et al. (1982) that a monument (mound 25, p. 266) within this group has the same orientation and silhouette as the Tacaná volcanic complex. If this mound was built in homage to the volcano, offerings strengthen our idea that Izapa villagers periodically returned to the vicinity. Recent studies of the orientation of

the monuments (mounds) at Izapa reveal that they were directly aligned toward the volcano (Gomez, 1996), further strengthening the link between Izapa and a cult honoring the volcano.

Future Hazards

Pyroclastic Flows and Landslides. During the late Pleistocene and Holocene, the Tacaná volcanic complex has erupted on several occasions, causing the destruction of summit domes and the subsequent formation of hot pyroclastic flows that have affected the surrounding area. These pyroclastic flows reached 10–15 km from the summit. The total population (Mexico-Guatemala) living within a 15 km radius from the summit is about 100 000 inhabitants. This population lives with the potential risk of a similar event from a future eruption of the volcano (Fig. 14A). The towns of La Vega del Volcán and San Rafael on the Guatemalan flank of the volcano are located at the intersection of the old caldera structure and the volcano apron at 3 and 3.5 km, respectively, from the summit. A laterally driven eruption similar to that of 1950 yr B.P. would easily reach these towns. In order to mitigate the effects of this scenario a seismic network to monitor the volcano is now being installed by the authorities of both countries.

Nevertheless, hazards posed by events that could occur with little warning can be envisaged. One of these is the instability of some sectors of the complex's main summit (i.e., Tacaná), which has a crater open towards the northwest filled by a main central dome. This crater scar has vertical walls, diverse hydrothermally altered areas, and in addition was the site of the phreatic explosion of 1986, which still contains an active fumarole. The Mexican town of Agua Caliente (population of 500) is located within the area subject to such a hazard (Fig. 14A).

Muddy Floods. Mudflows caused by volcanic activity, hurricane-related precipitation, landslides, or even landslide damming of rivers probably represent the most common and hazardous events that can be expected to affect the areas surrounding the volcano. All small tributaries and main rivers drain toward the Mexican side in their course toward the Pacific Ocean. This drainage network has formed two huge sedimentary aprons of fluviatile and lahar origin. These lowlands are the sites of several population centers, including the city of Tapachula (~250 000 habitants), and constitute the best agricultural lands in the region. The area includes the most important routes of communication to central Mexico and Central America (Fig. 14B).

We mentioned the series of mudflows in September 1998, which killed more than 150 people, and destroyed several towns and important portions of the Pan-American Highway. Immediate consequences of this catastrophic event were starvation and disease, mainly among the large, youthful population. The geological record of the area suggests that the 1998 event represents the latest of a series of geologically frequent disasters in the region. Renewed eruptive activity at the Tacaná volcanic complex and its effects on the drainages of the area, could, because of the large and rapidly increasing population, have a truly catastrophic impact.

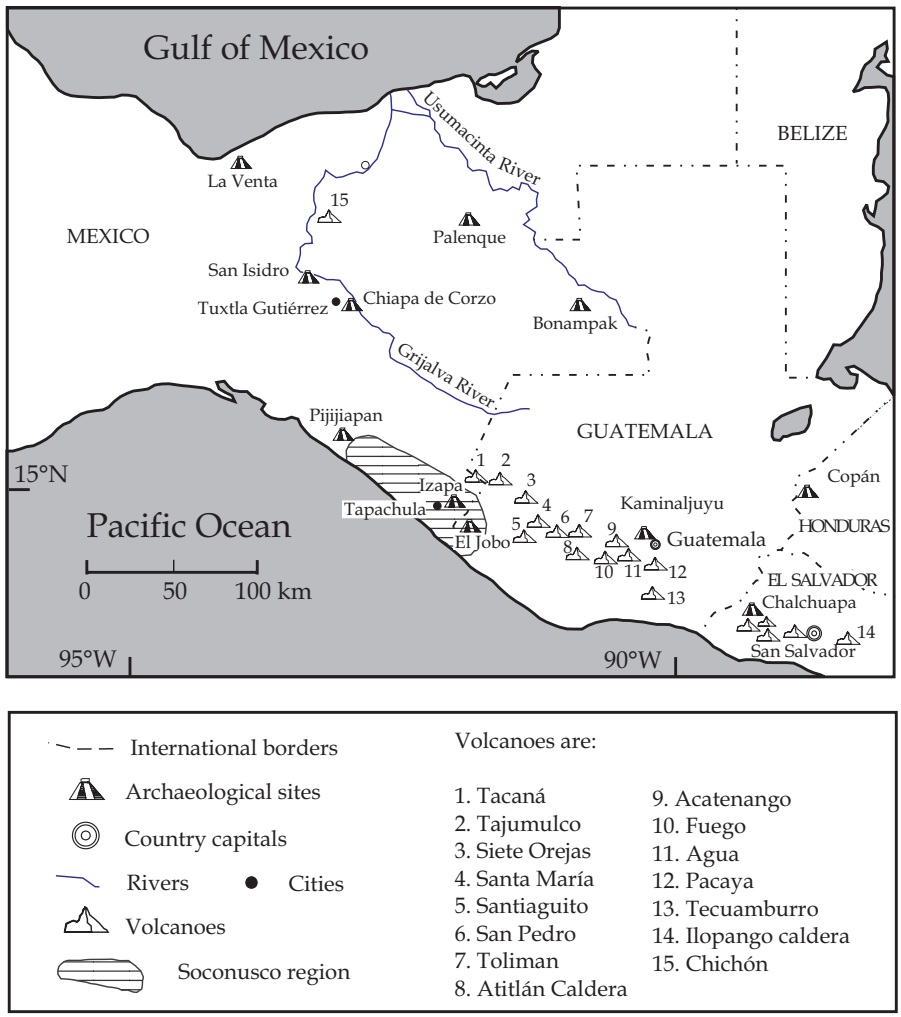

Figure 12. Sketch map of the location of main volcanoes in Central America. Relevant archaeological sites to this study such as Izapa, Kaminaljuyu, and Chalchuapa are indicated.

CONCLUSIONS

The Tacaná volcanic complex has undergone intense Holocene volcanic activity that was poorly understood despite the fact that the volcano has long been considered active. A magma-mixing process caused by the intrusion of a basic magma into an andesitic reservoir initiated a Peléan-style eruption from the southern sector of the San Antonio volcano. The event produced a series of block and ash flows that traveled about 14 km, covering an area of 25 km^2 and depositing a minimum volume of 0.12 km^3. Important secondary flooding took place along main drainages. Radiocarbon dating of four charcoal samples found within the deposit yielded an age of ca. 1950 yr B.P. This date matches a halt in the construction activity at Izapa, the most important cultural center in the Soconusco region at that time. Currently, an estimated 60 000 people live directly on the Mixcun flow deposit. Therefore, a future eruption, even of small magnitude, could pose a serious risk to the lives and property of

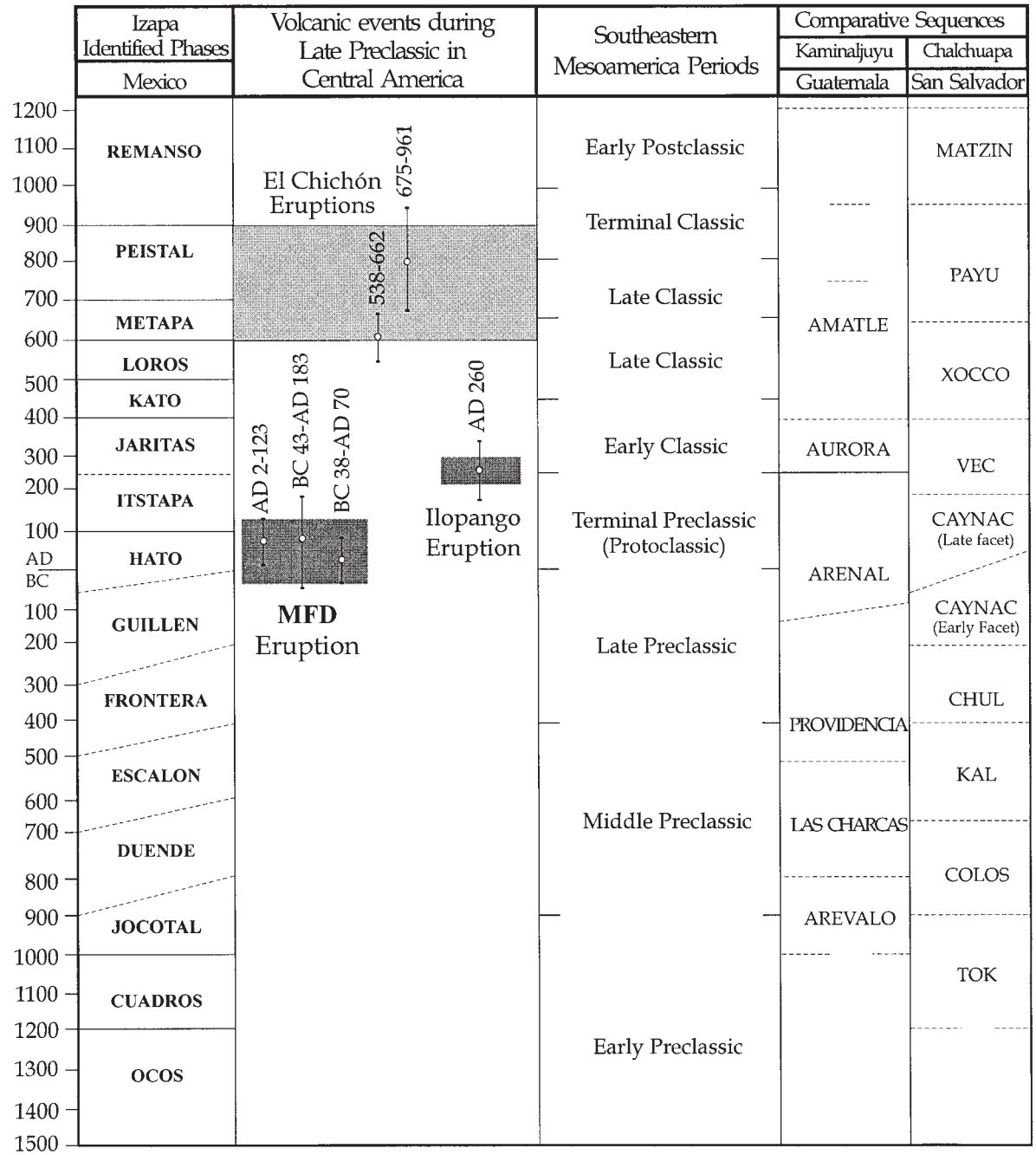

Figure 13. Chronological evolution of pre-Hispanic cultures in southern Mexico and Guatemala compiled from Lowe et al. (1982) and Sheets (1983). The light gray box indicates the period in which volcanic ash was used as a temper in vessels of the Maya lowlands (Ford and Rose, 1995). These authors proposed volcanoes in the Tacaná–Cerro Quemado region and El Chichón as the possible sources of ash fallout into the Maya lowlands. Espíndola et al. (2000) described two explosive eruptions of El Chichón volcano at 1250 and 1500 B.P. (A.D. 553–614 and A.D. 676–788, respectively), strengthening its candidacy as an ash supplier since those eruptions occurred within the A.D. 600–900 period. MFD-Mixcun flow deposit.

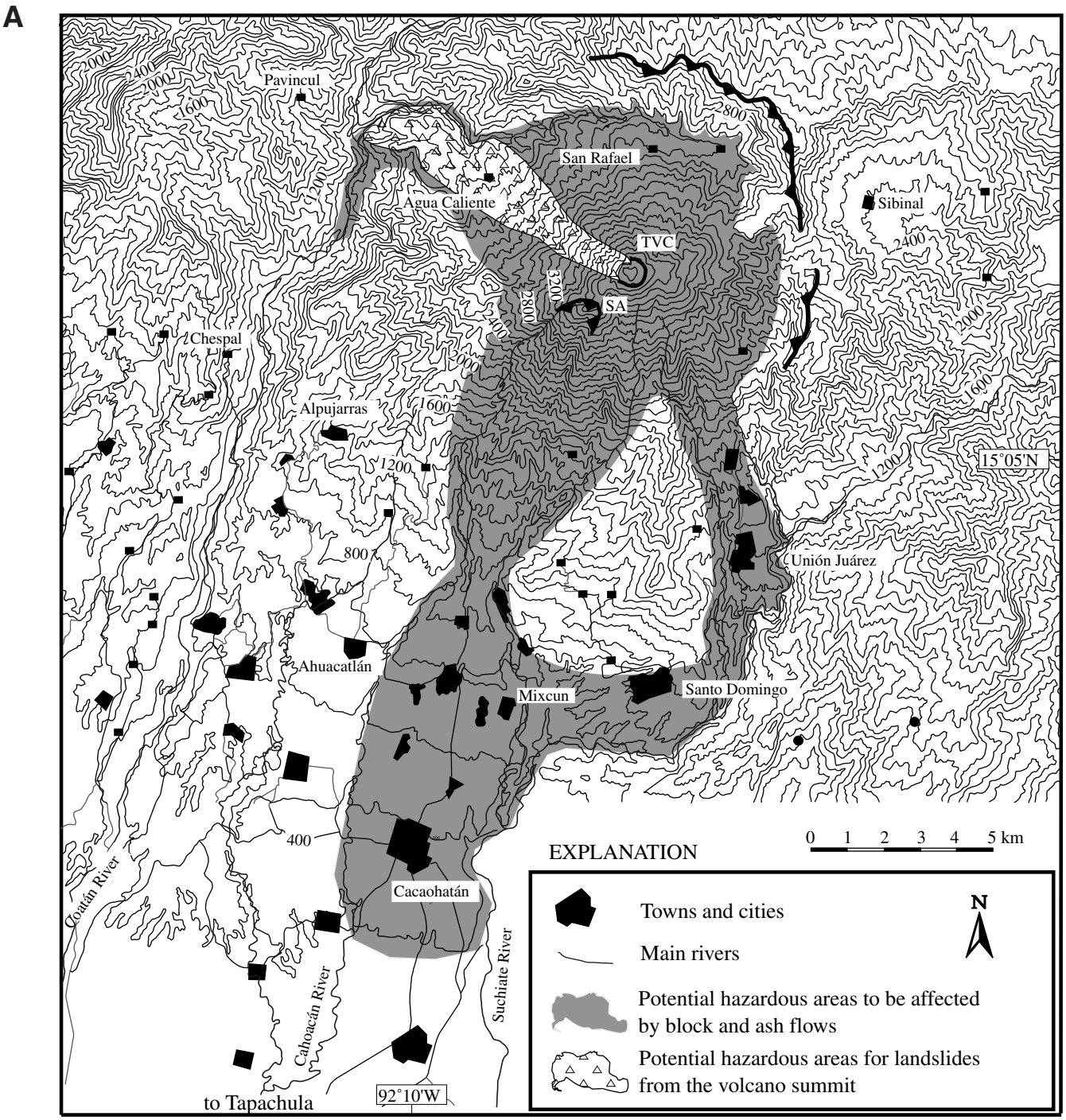

Figure 14. Hazards map of (A) pyroclastic flows produced by central dome explosions based on four recognized events during the past 40 k.y., and small-size landslides produced by flank instability, and (B) debris and hyperconcentrated flows produced by syneruptive or posteruptive processes.

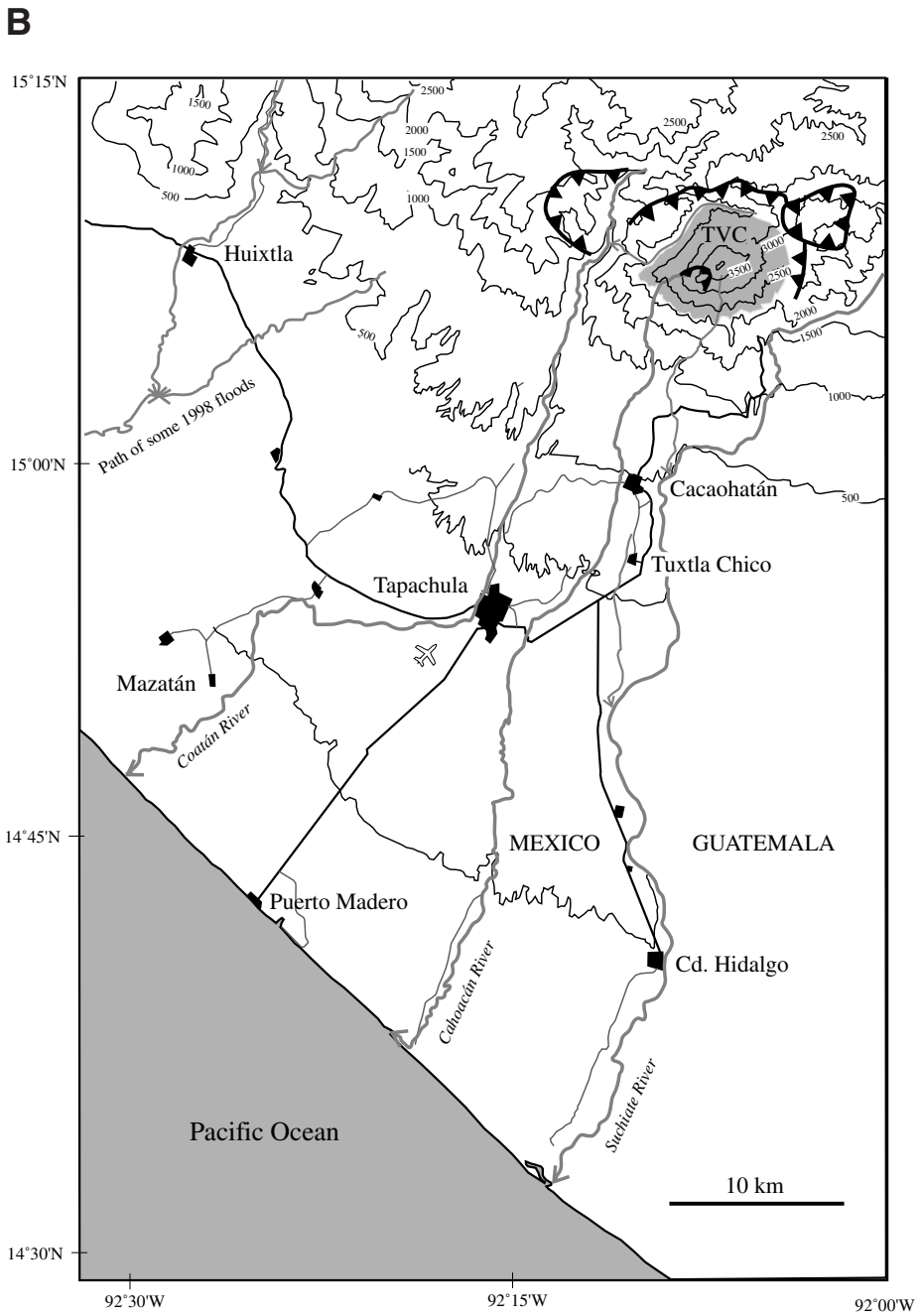

Figure 14. (*Continued*.)

thousands of people. Secondary flooding could also pose a threat to the 250 000 inhabitants in the city of Tapachula.

ACKNOWLEDGMENTS

This project was supported by grants from Instituto Panamericano de Geografía e Historia (3.4.3.30), Consejo National de Ciencia y Tecnología (27993T), Centro Nacional de Prevención de Desastres (PE–08), and the University of Florence, Italy, through N. Coradossi, P. Manetti, and O. Vaselli. F. Olmi provided technical support during the microprobe analyses performed at the University of Florence. We thank Y. Tarán, N. Varley, O. Matias, J. Calderón, and F. Boj who spent several days with us during our field work seasons. We are indebted to B. Voorhies and J. Robles, who provided us with relevant archaeological information of the Soconusco region. Jack McGeehin performed dating of some of the ^{14}C samples at the U.S. Geological Survey, Reston, Virginia. Reviews by M. Bursik, C. Chesner, B. Rose, and M. Carr greatly improved the ideas stated in this manuscript. We are also indebted to L. Caballero, K.E. Cervantes, and L. Capra, who drafted some of the figures.

REFERENCES CITED

Bacon, C.R., 1986, Magmatic inclusions in silicic and intermediate volcanic rocks: Journal of Geophysical Research, v. 91B, p. 6091–6112.

Bacon, C.R., and Metz, J., 1984, Magmatic inclusions in rhyolites, contaminated basalts, and compositional zonation beneath the Coso volcanic field, California: Contributions to Mineralogy and Petrology, v. 85, p. 346–365.

Bergeat, A., 1894, Zur Kenntnis der jungen Eruptivgesteine der Republik Guatemala: Zeitschrift der Deutschen Geologischen Gesellschaft, Berlin, p. 131–157.

Blake, M., Clark, J.E., Voorhies, B., Love, M., Pye, M., Demarest, A.A., and Arroyo, B., 1995, A revised chronology for the Late Archaic and Formative periods along the Pacific coast of southeastern Mesoamerica: Ancient Mesoamerica, v. 6, p. 1–183.

Blundy, J.D., and Sparks, R.S.J., 1992, Petrogenesis of mafic inclusions in granitoids of the Adamello Massif: Journal of Petrology, v. 104, p. 208–214.

Böse, E., 1903, Los temblores de Zanatepec, Oaxaca, a fines de septiembre de 1902. Estado actual del volcán Tacaná, Chiapas, México. Oficina tipográfica de la Secretaría de Fomento: Parergones, Instituto Geológico, no. 1, 25 p.

Boudon, G., Camus, G., Gourgaud, A., and Lajoie, J., 1993, The 1984 nuée-ardente deposits of Merapi volcano, Central Java, Indonesia: Stratigraphy, textural characteristics, and transport mechanisms: Bulletin of Volcanology, v. 55, p. 327–342.

Bourdier, J.L., Boudon, G., and Gourgaud, A., 1989, Stratigraphy of the 1902 and 1929 nuée-ardente deposits, Mt. Pelée, Martinique: Journal of Volcanology and Geothermal Research, v. 38, p. 77–96.

Cole, P.D., Calder, E.S., Druitt, T.H., Hoblitt, R., Robertson, R., Sparks, R.S.J., and Young, S.R., 1998, Pyroclastic flows generated by gravitational instability of the 1996–1997 lava dome of Soufrière Hills Volcano, Montserrat: Geophysical Research Letters, v. 25, p. 3425–3428.

Conway, F.M., Vallance, J.W., Rose, W.I., Johns, G.W., and Paniagua, S., 1992, Cerro Quemado Guatemala: The volcanic history and hazards of an exogenous volcanic dome complex: Journal of Volcanology and Geothermal Research, v. 52, p. 303–323.

De Cserna, Z., Aranda-Gómez, J.J., and Mitre, L.M., 1998, Mapa fotogeológico preliminar y secciones estructurales del Volcán Tacaná: Universidad Nacional Autónoma de México, Instituto de Geología, 1 map, Cartas Geológicas y Mineras de la República Mexicana, scale 1:50 000.

De la Cruz, V., and Hernández, R., 1985, Estudio geológico a semidetalle de la zona geotérmica del Volcán Tacaná, Chiapas: Mexico, Comisión Federal de Electricidad, 41/85, 30 p.

De la Cruz-Reyna, S., Armienta, M.A., Zamora, V., and Juárez, F., 1989, Chemical changes in spring waters at Tacaná Volcano, Chiapas, México: Journal of Volcanology and Geothermal Research, v. 38, p. 345–353.

Eichelberg, J.C., 1978, Andesitic volcanism and crustal evolution: Nature, v. 275, p. 21–27.

Eichelberg, J.C., 1980, Vesiculation of mafic magma during replenishment of silicic magma reservoirs: Nature, v. 288, p. 446–450.

Espíndola, J.M., Medina, F.M., and De los Ríos, M., 1989, A C–14 age determination in the Tacaná volcano (Chiapas, Mexico): Geofisica Internacional, v. 28, p. 123–128.

Espíndola, J.M., Macías, J.L., and Sheridan, M.F., 1993, El Volcán Tacaná: Un ejemplo de los problemas en la evaluación del Riesgo Volcánico, *in* Proceedings, Simposio Internacional sobre Riesgos Naturales e Inducidos en los

Grandes Centros Urbanos de America Latina: México D.F., Centro Nacional de Prevención de Desastres, p. 62–71.
Espíndola, J.M., Macías, J.L., Tilling, R.I., and Sheridan, M.F., 2000, Volcanic history of El Chichón Volcano (Chiapas, México) during the Holocene, and its impact on human activity: Bulletin of Volcanology (in press).
Folk, R.L., and Ward, W.C., 1957, Brazos river bar: A study of the significance of grain size parameters: Journal of Sedimentary Petrology, v. 27, p. 3–26.
Ford, A., and Rose, W.I., 1995, Volcanic ash in ancient Maya ceramics of the limestone lowlands: Implications for prehistoric activity in the Guatemala Highlands: Journal of Volcanology and Geothermal Research, v. 66, p. 149–162.
Francalanci, L., 1987, Evoluzione vulcanologica e magmatologica di Stromboli (Isole Eolie): Relazione tra magmatismo calc-alcalino e shoshonitico [Ph.D. dissert.]: Firenze, Italia, Università degli Studi di Firenze, 329 p.
Gill, J.B., 1981, Orogenic andesites and plate tectonics: Berlin, Springer-Verlag, 358 p.
Gomez, H.R., 1996, Izapa, organización espacial de un centro del Formativo en la costa pacífica de Chiapas, *in* Proceedings, IX Simposio de investigaciones arqueológicas: Guatemala, Guatemala, Museo Nacional de Arqueología y Etnología, p. 549–563.
Halsor, S.P., 1989, Large glass inclusions in plagioclase phenocrysts and their bearing on the origin of mixed andesites lavas at Tolimán Volcano, Guatemala: Bulletin of Volcanology, v. 51, p. 271–280.
Halsor, S.P., and Rose, W.I., 1988, Common characteristics of paired volcanoes in northern Central America: Journal of Geophysical Research, v. 93, p. 4467–4476.
Hart, W.J.E., and Steen-McIntyre, V., 1983, Tierra Blanca Joven Tephra from the A.D. 260 eruption of Ilopango caldera, *in* Sheets, P.D., ed., Archaeology and volcanism in Central America. The Zapotitlán Valley of El Salvador: Austin, University of Texas, The Texas Pan American series, p. 14–34.
Heiken, G., and Eichelberg, J.C., 1980, Eruptions at Chaos Crags, Lassen Volcanic National Park, California: Journal of Volcanology and Geothermal Research, v. 7, p. 443–481.
Irvine, T.N., and Baragar, W.R.A., 1971, A guide to the chemical classification of the common rocks: Canadian Journal of Earth Sciences, v. 8, p. 523–548.
Kouchi, A., and Sunagawa, I., 1985, A model for mixing basaltic and dacitic magmas as deduced from experimental data: Contributions to Mineralogy and Petrology, v. 89, p. 17–23.
Koyaguchi, T., 1986, Textural and compositional evidence for magma mixing and its mechanism, Abu volcano group, Southwestern Japan: Contributions to Mineralogy and Petrology, v. 93, p. 33–45.
Lowe, G.W., 1977, The Mixe-Zoque as competing neighbors of the early Lowland Maya, *in* Adams, R.E.W., ed., The origins of Maya civilization: Albuquerque, University of New Mexico Press, p. 197–248.
Lowe, G.W., Lee, T.A., and Martínez-Espinosa, E., 1982, Izapa: An introduction to the ruins and monuments: Provo, Utah, Brigham Young University, Papers of the New World Archaeological Foundation, no. 31, 439 p.
Macías, J.L., Espíndola, J.M., Bursik, M., and Sheridan, M.F., 1998, Development of lithic-breccias in the 1982 pyroclastic flow deposits of El Chichón Volcano, Mexico: Journal of Volcanology and Geothermal Research, v. 83, p. 173–196.
Matsuwo, T.U.N., Sumita, M., Fujinawa, A., Sato, H., and Takarada, S., 1997, Diversity of block-and-ash flow generations during the 1990–96 eruption of Unzen Volcano, *in* Nakada, S., Eichelberg, J., and Shimizu, H., eds., Unzen International Workshop: Shimibara, Japan, Decade Volcano and Scientific Drilling, Volcanology Society of Japan, p. 26–27.
Mellors, R.A., Waitt, R.B., and Swanson, D.A., 1988, Generation of pyroclastic flows and surges by hot-rock avalanches from the dome of Mount St. Helens volcano, USA: Bulletin of Volcanology, v. 50, p. 14–25.
Mercado, R., and Rose, W.I., 1992, Reconocimiento geológico y evaluación preliminar de peligrosidad del Volcán Tacaná, Guatemala/México: Geofisica Internacional, v. 31, p. 205–237.
Michaels, G.H., and Voorhies, B., 1999, Late Archaic period coastal collectors in southern Mesoamerica; The Chantuto People revisited, *in* Blake, M., ed., Pacific Latin America in prehistory: Pullman, Washington, State University Press, The evolution of archaic and formative cultures, p. 39–54.
Moore, J.G., and Melson, W.G., 1969, Nuées ardentes of the 1968 eruption of Mayon Volcano, Philippines: Bulletin of Volcanology, v. 33, p. 600–620.
Mujica, R., 1987, Estudio petrogenético de las rocas ígneas y metamórficas en el Macizo de Chiapas: Instituto Mexicano del Petróleo, Reporte Interno C-2099, p. 47.
Müllerried, F.K.G., 1951, La reciente actividad del Volcán de Tacaná, Estado de Chiapas, a fines de 1949 y principios de 1950: Informe del Instituto de Geología de la Universidad Nacional Autónoma de México, p. 28.
Murphy, M.D., Sparks, R.S.J., Barclay, J., Carroll, M.R., Lejeune, A.-M., Brewer, T.S., Macdonald, R., Black, S., and Young, S., 1998, The role of magma mixing in triggering the current eruption at the Soufrière Hills volcano, Montserrat, West Indies: Geophysical Research Letters, v. 25, p. 3433–3446.
Nairn, I.A., and Self, S., 1978, Explosive eruptions and pyroclastic avalanches from Ngauruhoe in February 1976: Journal of Volcanology and Geothermal Research, v. 3, p. 39–60.
Rodríguez-Elizarrarás, S., Siebe, C., Komorowski, J.-C., Espíndola, J.M., and Saucedo, R., 1991, Field observations of pristine block-and-ash flow deposits emplaced April 16–17, 1991 at Volcán de Colima, Mexico: Journal of Volcanology and Geothermal Research, v. 48, p. 399–412.
Rose, W.I., 1972, Notes on the 1902 eruption of Santa María volcano, Guatemala: Bulletin of Volcanology, v. 36, p. 29–45.
Rose, W.I., Pearson, T., and Bonis, S., 1976–1977, Nuée ardente eruption from the foot of a dacite lava flow, Santiaguito volcano, Guatemala: Bulletin of Volcanology, v. 40, p. 23–38.
Sakuyama, M., 1984, Magma mixing and magma plumbing systems in Island Arcs: Bulletin of Volcanology, v. 47, p. 685–703.
Sapper, C., 1927, Vulkankunde: Stuttgart, Germany, J. Engelhorns Nachfahren, 424 p.
Sawlan, M.G., 1986, Petrogenesis of late Cenozoic volcanic rocks from Baja California Sur, Mexico [Ph.D. thesis]: Santa Cruz, University of California, 174 p.
Scott, K.M., Vallance, J.W., and Pringle, P.T., 1995, Sedimentology, behavior and hazards of debris flows at Mount Rainier, Washington: U.S. Geological Survey Professional Paper 1547, p. 56.
Seymour, K.S., and Vlassopoulos, D., 1992, Magma mixing at Nysiros volcano, as inferred from incompatible trace-elements systematics: Journal of Volcanology and Geothermal Research, v. 50, p. 273–299.
Sharer, R.J., 1974, The prehistory of the southeastern Maya periphery: Current Anthropology, v. 15, no. 2, p. 165–187.
Sharer, R.J., 1978, The pottery of Chalchuapa, El Salvador, *in* Sharer, R.J., ed., The prehistory of Chalchuapa, El Salvador: Philadelphia, University of Pennsylvania Press, v. 1, p. 218–226.
Sheets, P.D., 1971, An ancient natural disaster: Expedition, v. 14, p. 25–31.
Sheets, P.D., 1976, The terminal pre-classic lithic industry of the southern Maya highlands: A component of the proto-classic site-unit intrusions in the lowlands?, *in* Proceedings, Belize Field Symposium, Maya Lithic Studies: San Antonio, University of Texas, Center for Archaeological Research, p. 55–69.
Sheets, P.D., 1983, Introduction, *in* Sheets, P.D., ed., Archaeology and volcanism in Central America. The Zapotitlán Valley of El Salvador: Austin, University of Texas Press, p. 1–13.
Stuiver, M., and Reimer, J., 1986, Extended ^{14}C data base and revised CALIB 3.0 calibration program: Radiocarbon, v. 28, p. 215–230.
Voorhies, B., 1989, An introduction to the Soconusco and its prehistory, *in* Voorhies, B., ed., Economies of the Soconusco region of Mesoamerica. Ancient trade and tribute: Salt Lake City, University of Utah Press, p. 1–18.
Voorhies, B., and Kennett, D., 1995, Buried sites on the Soconusco coastal plain, Chiapas, Mexico: Journal of Field Archaeology, v. 22, p. 65–79.
Voorhies, B., 2000, Informe Final de las Investigaciones en Cerro de las Conchas, Municipio de Huixtla, Chiapas: Reporte Interno, Submitted to the Instituto Nacional de Antropología e Historia, México.
Williams, S.N., and Self, S., 1983, The October 1902, Plinian eruption of Santa María Volcano, Guatemala: Journal of Volcanology and Geothermal Research, v. 16, p. 33–56.
Wood, D.A., 1979, A variably veined suboceanic upper mantle. Genetic significance for mid-ocean ridge basalts from geochemical evidences: Geology, v. 7, p. 499–503.

MANUSCRIPT RECEIVED BY THE SOCIETY APRIL 9, 1999
REVISED MANUSCRIPT RECEIVED DECEMBER 20, 1999
MANUSCRIPT ACCEPTED DECEMBER 21, 1999

Printed in USA